Geomorphology xxx (2011) xxx–xxx

Contents lists available at ScienceDirect

Geomorphology

journal homepage: www.elsevier.com/locate/geomorph

Preservation of beach ridges due to pedogenic calcrete development in the Tongoy palaeobay, North-Central Chile

Marco Pfeiffer [a,b,*], Jacobus P. Le Roux [a], Elizabeth Solleiro-Rebolledo [c], Helga Kemnitz [d], Sergey Sedov [c], Oscar Seguel [b]

[a] Departamento de Geología, Facultad de Ciencias Físicas y Matemáticas, Universidad de Chile, Plaza Ercilla 803, 8370450 Santiago, Chile
[b] Departamento de Ingeniería y Suelos, Facultad de Ciencias Agronómicas, Universidad de Chile, Santa Rosa 11315, 8820808 La Pintana, Chile
[c] Instituto de Geología, Universidad Nacional Autónoma de México, Del. Coyoacán 04510 D.F. Mexico
[d] Helmholtz Center Potsdam, Deutsches GeoForschungsZentrum, Section 3.1, Telegrafenberg, 14473, Germany

ARTICLE INFO

Article history:
Received 25 October 2010
Received in revised form 9 May 2011
Accepted 15 May 2011
Available online xxxx

Keywords:
Calcrete
Beach ridge
Petrocalcic horizon
Marine terrace
Pedogenesis
Tongoy

ABSTRACT

At the Tongoy palaeobay in north-central Chile, a series of beach ridges developed during seaward progradation that took place after the MIS 11 sea-level highstand (412 ka). The microrelief left by this succession of beach ridges has been well preserved from erosion due to the development of a calcrete (petrocalcic horizons), which was resistant to the chemical and physical weathering that characterized the area during humid phases of the late Pleistocene and middle Holocene. Macro- and micro-morphological analysis shows that the calcrete is of pedogenic origin and formed during two stages: in the first stage a massive (beta) calcrete developed, followed during the second stage by a laminar (alpha) calcrete. Each event in the development of the calcrete was intimately related to the foregoing process, mainly due to changes in the permeability of the profile horizons. During the first stages of development, organisms played an important role in the precipitation of calcite, which made the calcrete less permeable and favored the accumulation of ponded water during the wet season. As a result of this increased humidity, calcium carbonate with a laminar structure was precipitated. The development of the calcrete was also intimately associated with the evolution of the drainage network, which is characterized by a trellis pattern of tributaries parallel to the beach ridges. This study demonstrates the importance of soil genesis in the geomorphological evolution of landscapes.

1. Introduction

Soils result from the interaction of factors such as climate, vegetation, topographic setting, parent material, and time (Jenny, 1980; Birkeland, 1999). Because soil development can affect the properties of unconsolidated deposits (Birkeland, 1999) it can influence the hydrological and erosional processes that occur during landscape evolution (Dunne, 1978; Wells et al., 1987; McAuliffe, 1994; Eppes et al., 2002). This is particularly true for indurated horizons such as calcretes (petrocalcic horizons), which increase drainage and runoff due to making the soil profile impermeable, and also diminish erosion rates because of their mechanical resistance. For example, Eppes et al. (2002) discussed the role that soil played in the topographic evolution of the San Bernardino Mountains in California, where the development of a petrocalcic horizon preserved prominent ridges formed by anticlinal folds due to its high resistance to erosion. Another example occurs in the southern Pampean landscape of Argentina, where a petrocalcic horizon constituted a resistant surface that survived a series of erosional cycles and preserved an undulating, early Pleistocene topography (Amiotti et al., 2001; Blanco and Stoops, 2007). More examples of calcrete protection from erosion can be found in Arizona at the Mormon Mesa (Brock and Buck, 2009) and Buckeye (VanArsdale, 1982). Therefore, a close relationship exists between geomorphology and soil development, and soil evolution can elucidate the development of a particular landscape. In this study we examine the relationship between soil formation and the preservation of Pleistocene beach ridges south of La Serena, north-central Chile (Fig. 1).

Pleistocene beach ridges are uncommon features in the stratigraphic record, their preservation occurring mostly in arid climates where the effect of erosion is more limited (Augustinus, 1989; Meldahl, 1995; Otvos, 2000). Along the Chilean coastline, Pleistocene beach ridges are preserved in the hyper-arid Atacama desert (Armijo and Thiele, 1990; Marquardt et al., 2004; Victor et al., 2011), whereas in the more humid

* Corresponding author at: Departamento de Geología, Facultad de Ciencias Físicas y Matemáticas, Universidad de Chile, Plaza Ercilla 803, 8370450 Santiago, Chile. Tel.: +56 2 9784123.
E-mail addresses: mpfeiffer@ug.uchile.cl (M. Pfeiffer), jroux@cec.uchile.cl (J.P. Le Roux), solleiro@geologia.unam.mx (E. Solleiro-Rebolledo), heke@gfz-potsdam.de (H. Kemnitz), sergey@geologia.unam.mx (S. Sedov), oseguel@uchile.cl (O. Seguel).

0169-555X/$ – see front matter © 2011 Elsevier B.V. All rights reserved.
doi:10.1016/j.geomorph.2011.05.012

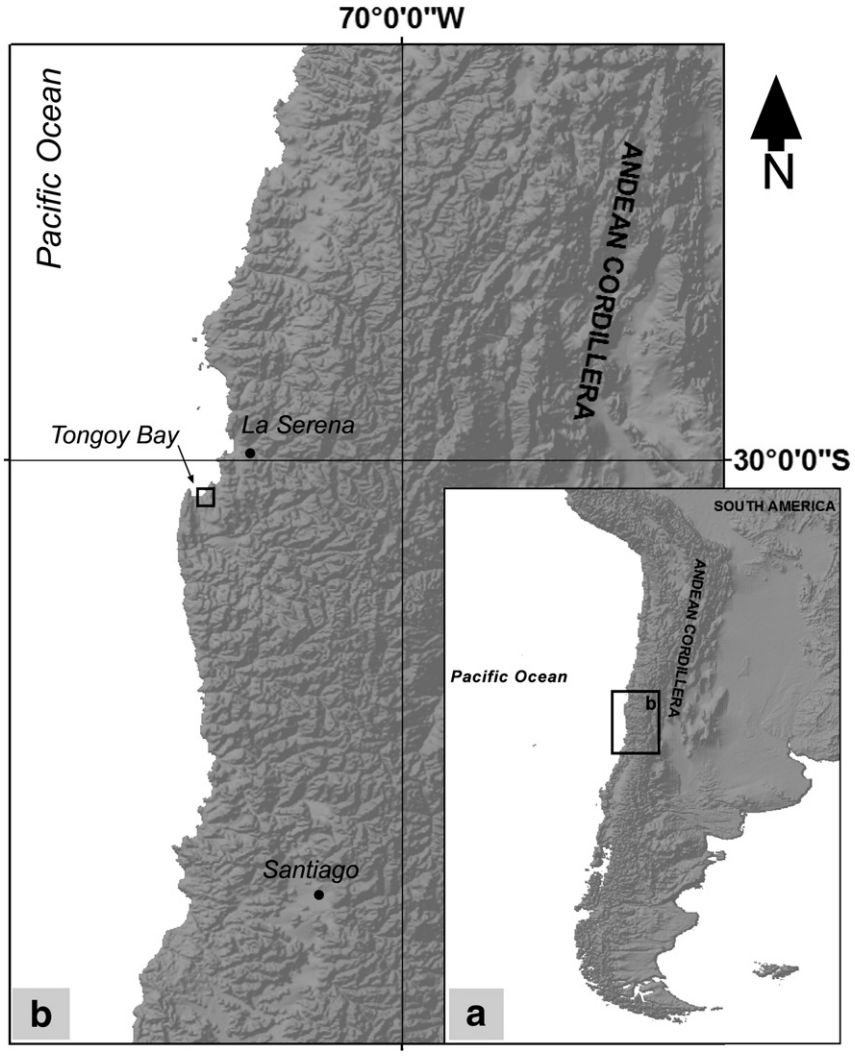

Fig. 1. (a) Location of the study area superimposed on a Digital Elevation Model of southern South America (b) Close-up of rectangle shown in (a), rectangle corresponds to Fig. 2a.

south only Holocene beach ridges have been documented (Nelson and Manley, 1992; Bookhagen et al., 2006; Melnick et al., 2006). In Argentinian Patagonia, Holocene and Pleistocene shoreline sequences are also preserved, but the latter are scarcer because of probable erosion (Schellmann and Radtke, 2010; Pedoja et al., 2011).

In the Tongoy palaeobay, a series of marine terraces described by several authors (Darwin, 1846; Domeyko, 1848; Brüggen, 1950; Chávez, 1967; Herm, 1969; Paskoff, 1970; Ota et al., 1995; Benado, 2000; Heinze, 2003; Saillard, 2008) developed over marine deposits corresponding to the Mio–Pleistocene Coquimbo Formation (Le Roux et al., 2006). One of these terraces reaches more than 30 km in its widest section. It was dated by Saillard (2008) using U-Th dating on marine shells, which yielded an age of around 400 ka corresponding to Marine Isotopic Stage (MIS) 11. Upon this extensive platform a pedogenic calcrete was formed after the marine regression that followed the MIS 11 highstand (Paskoff, 1970; Vera, 1985; Saillard, 2008).

The development of calcrete can be of diagenetic or pedogenic origin (Wright and Tucker, 1991), the latter implying surface processes so that plants and other organisms can participate in their formation. Calcretes normally experience several stages of development that correspond to different environmental conditions (Gile et al., 1966; Machette, 1985; Wright and Tucker, 1991; Alonso-Zarza and Wright, 2010; Gallala et al., 2010). The Tongoy calcrete shows the most advanced stage (VI) of development according to Machette (1985), which implies a series of processes during its evolution. In this paper we propose a model for the development of the Tongoy calcrete, based on micro- and macro-morphological features, soil chemistry and geomorphological analysis.

2. Geographic, geological and geomorphological setting

The study area is located south of the Bay of Tongoy, at 30°18´S 71°33´W, 40 km south of the city of La Serena and 430 km north of Santiago (Fig. 1). Although the climate is semi-arid, prolonged multi-year droughts or extremely rainy seasons occur, with occasional intense rainfall or even debris flow events (Vargas et al., 2006). The area has also been described as having a Mediterranean climate because 85.7% of the average annual precipitation is concentrated in the winter months (May–August), while the summer is very dry; the mean annual precipitation lying between 75 and 100 mm, and the mean annual temperature being 13.6 °C (CIREN, 1990).

The dominant vegetation is composed of steppe forest, i.e. low shrubs, small trees and different herbaceous species adapted to dry conditions (Gajardo, 1994).

The Coquimbo Formation is composed of shallow marine or bayfill deposits including mudstones, sandstones, coquinas and conglomerates that accumulated during a series of transgressions and regressions related to regional and local tectonic movements combined with global sea-level variations (Le Roux et al., 2006). The succession

Please cite this article as: Pfeiffer, M., et al., Preservation of beach ridges due to pedogenic calcrete development in the Tongoy palaeobay, North-Central Chile, Geomorphology (2011), doi:10.1016/j.geomorph.2011.05.012

developed within a tectonic semi-graben (Paskoff, 1970; Heinze, 2003) formed to the east of the Puerto Aldea Fault, which brings the Coquimbo Formation in contact with Triassic–Jurassic intrusives (Emparan and Pineda, 2006).

Olivares (2004) and Le Roux et al. (2006) described a series of detailed stratigraphic columns of the Coquimbo Formation in the Tongoy area and proposed a correlation between facies sequences and marine oscillations. Six marine transgressions were identified, the first occurring between 11.9 and 11.2 Ma and the last between 1.7 and 1.4 Ma. This variation of the relative sea level continued during the Pleistocene, leaving a series of wave-cut terraces upon the Coquimbo Formation (Ota et al., 1995; Saillard, 2008). These terraces were identified for the first time by Darwin (1846) and studied in detail by Ota et al. (1995), who identified four terraces in the Tongoy area, designated T_I–T_{IV} in order of decreasing age. In a later study, Benado (2000) also identified the lowest Holocene level as a terrace. T_I only appears in the Altos de Talinay area, whereas the oldest terrace recognized in the Tongoy palaeobay area is T_{II} (Fig. 2). Ota et al. (1995) assigned T_{II} to MIS 9 based on geomorphological correlation with terraces at the Bay of Coquimbo to the north, which were dated using U-series on shells by Radtke (1989). However, Saillard (2008), employing U-Th dating on shells from three beach ridges associated with the T_{II} terrace, assigned it to MIS 11, around 412 ka according to the eustatic curve of Siddall et al. (2006). Regard et al. (2010) attributed this terrace to a wide planar feature that occurs in many localities along the Pacific Coast between 15° and 30°S, revealing a period of uplift quiescence between the late Pliocene and MIS 11.

Upon T_{II}, a series of lines parallel to the shoreline can be observed on satellite images (Fig. 3), which are beach ridges corresponding to the last marine regression that affected this surface (Paskoff, 1970). These deposits where described by Paskoff (1970) as lumachella and coquina composed of carbonate-cemented shell fragments, subsequently covered by thin aeolian deposits. This succession reaches a maximum thickness of about 25 m in a road cut near Tongoy (Paskoff, 1970). Olivares (2004) also described coquinas associated with the marine regression that overlie older beach and upper to lower shoreface deposits of the Coquimbo Formation. Saillard (2008) attributed the presence of the beach ridges to shoreline stillstands during the progressive fall in sea level following the MIS 11 highstand.

3. Materials and methods

We studied three soil profiles developed over T_{II}, together with a published soil description by Aburto et al. (2008). The profiles are located at four points on terrace T_{II}, in a sequence that goes from the interior to the coast following the marine regression (Fig. 2a, b, c). This allows us to evaluate the soils in the entire prograding sequence at sample points located at 1.8 km (Tortolas), 4.2 km (Alamito), 8.0 km (La Montosa) and 12.2 km (Maitencillo) from the coast; Tortolas having the youngest surface exposure and Maitencillo the oldest (Fig. 2d). Observations were made in existing road cuts and limestone quarries as well as shallow trenches made by excavator. The macro-morphological soil characteristics were described according to the scheme proposed by Schoenberger et al. (2002).

We assume the soil age to be the time of bedrock exposure to the atmosphere (Jenny, 1941), in this case that of the Coquimbo Formation following the marine regression after MIS 11.

From each soil horizon bulk samples were taken for chemical, physical and micro-morphological analysis, while shells were collected for taxonomical identification. Undisturbed samples for thin sections

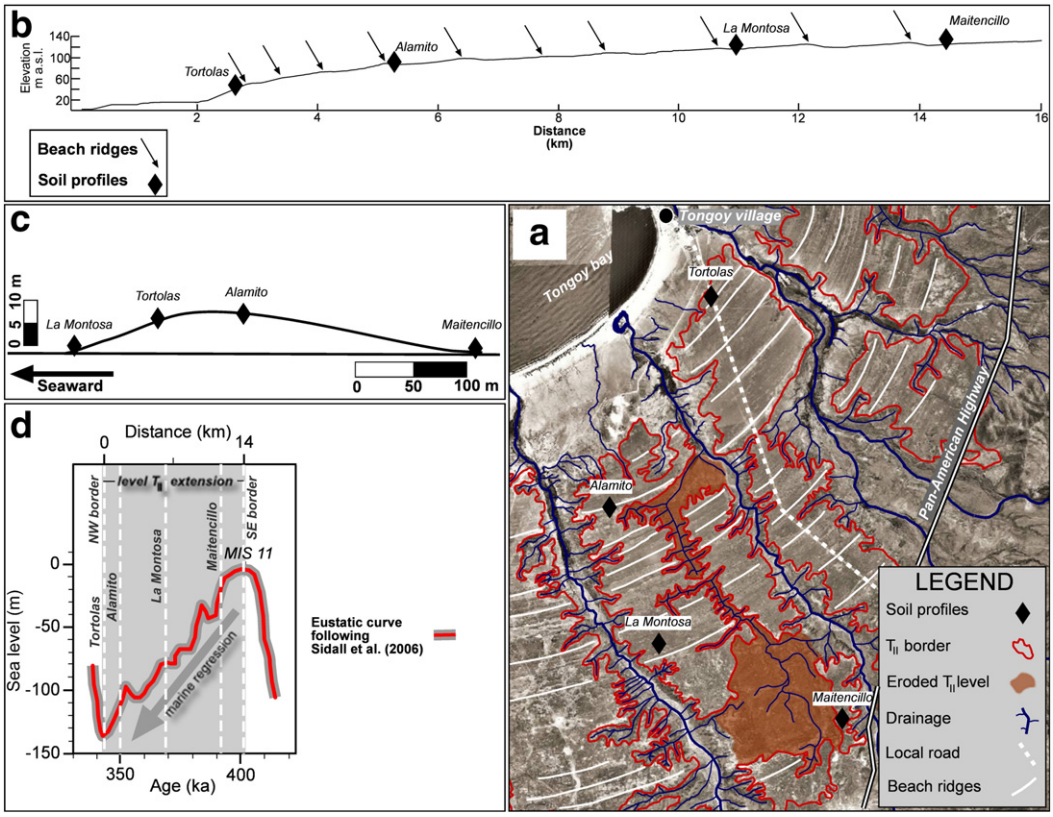

Fig. 2. (a) Aerial photograph of the study area (SAF 97 1:70,000, Ovalle L3, Nº 002945), showing the location of analyzed profiles in relation to geomorphic features. The profile presented in (b) corresponds to a local road section. (b) GPS profile modified after Saillard (2008). The individual profiles are shown in relation to their relative position in the general cross-section and not to their distances from the sea. (c) Relative position of soil profiles according to an "idealized" beach ridge representing the average dimensions of beach ridges and swales measured. (d) Sea-level variation around and after the MIS 11 sea-level highstand and the relative age of soil surface exposures of studied sites according to their relative positions.

Please cite this article as: Pfeiffer, M., et al., Preservation of beach ridges due to pedogenic calcrete development in the Tongoy palaeobay, North-Central Chile, Geomorphology (2011), doi:10.1016/j.geomorph.2011.05.012

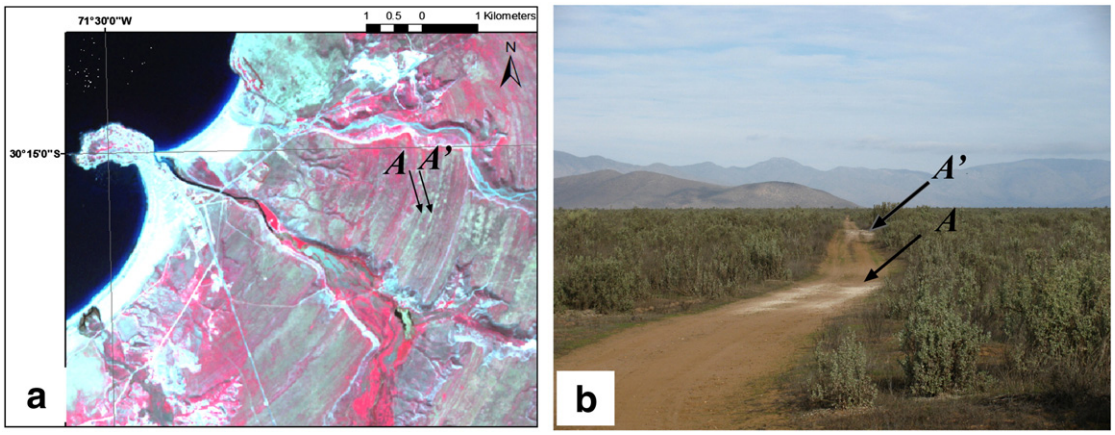

Fig. 3. (a) Satellite image ASTER (RGB: 321) showing concentric lines parallel to the shoreline and the location of photograph shown in (b). (b) Photograph taken on Tongoy T_{II} terrace showing the differences in soil surface color due to outcrops of calcrete in ancient beach ridge deposits.

were also collected from soil horizons, which were impregnated with resin and studied under a petrographic microscope. Descriptions follow the terminology proposed by Bullock et al. (1985), Wright and Tucker (1991), and Stoops (2003). Bulk density, electrical conductivity (EC), pH, organic matter (OM), extractable anions (HCO_3^-, Cl^-, SO_4^{2-}) and extractable cations (Na^+, K^+, Ca^{2+}, Mg^{2+}) were analyzed according to the methodology of Sadzawka et al. (2004).

Three topsoil samples (Alamito, La Montosa and Maitencillo) were selected for quartz grain surface analysis. About 100 g of each soil sample was treated as described by Krinsley and Donahue (1968).

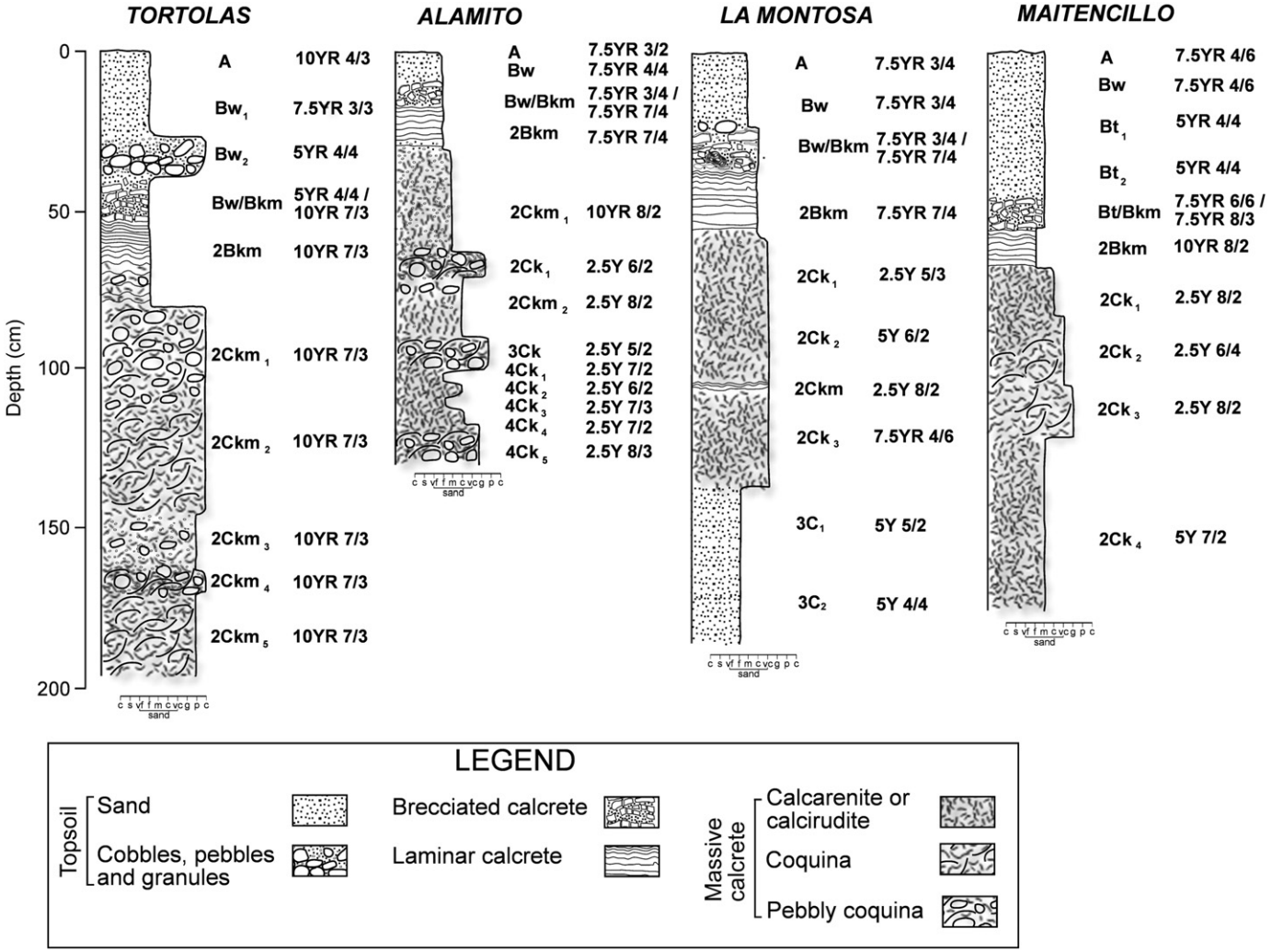

Fig. 4. Stratigraphic schemes of soil profiles with soil horizons and Munsell moist soil color. For horizon terminology see Appendix.

Please cite this article as: Pfeiffer, M., et al., Preservation of beach ridges due to pedogenic calcrete development in the Tongoy palaeobay, North-Central Chile, Geomorphology (2011), doi:10.1016/j.geomorph.2011.05.012

Possible veneers on the grain surfaces were removed by boiling in 18% hydrochloric acid. From the dried, sand-sized fraction, at least 50 grains were picked under a stereomicroscope and mounted on aluminum stubs. As all samples contained two different kinds of presumed quartz grains, each sample was divided into an (a)- and (b)-subsample, with (a) representing generally rounded, semi-transparent to frosty grains, and (b) being crystal clear to transparent, generally angular grains. The sample stubs were finally gold–palladium coated for examination under a scanning electron microscope (SEM; ZEISS Ultra 55 Plus) equipped with an energy-dispersive X-ray detector (EDS) using a silicon-drift detector and analytical software NSS by Thermo Fisher Scientific. A brief checking procedure using the EDS helped to exclude all non-quartz grains. A number assigned to each grain, indicated on an overlay on the SEM screen, allowed the individual grains to be tracked. Examination under the SEM also included documentation of the relative frequency (in percentage) of each grain micro-feature by visual estimation. These and all other micro-features, including their sequence relationships, were documented on working sheets and by micro-photographs.

4. Results

4.1. The prograding strandplain at Tongoy: main geomorphological features and processes

We assumed that the area covered by beach ridges on terrace T_{II} at Tongoy (Paskoff, 1970; Ota et al., 1995; Benado, 2000; Emparan and Pineda, 2006) was abraded during the last marine transgression of MIS 11 (Saillard, 2008). We attribute these features to have originated as beach berms, following Otvos (2000). According to this model, a beach ridge sequence in a progradational environment starts with a berm, a feature described by Hine (1979) as a shore-parallel linear body of triangular cross-section with a horizontal to slightly landward-dipping a surface (berm top) and a steeper seaward-dipping slope (beach face). When actively forming, a berm is situated between the foreshore and the landward (or lagoonward) margin of the backshore. The landward margin of such a ridge may be defined by the shoreline of an elongated shore-parallel lagoon or beach pond, enclosed during the growth of a shore-parallel spit. As a series of berm ridges prograde, shore-parallel swales bracket each ridge (Otvos, 2000).

At Tongoy, the beach ridges are mainly formed by marine shells that accumulated during marine transgression, which reworked deposits of the underlying Coquimbo Formation. The shelly deposits are capped by medium-grained sand (Paskoff, 1970). We identified a clear sequence of 11 beach ridges along the road that enters Tongoy Village from the Panamerican Highway on the T_{II} level (Fig. 2a). Although beach ridges normally have steep seaward slopes and more gentle landward slopes, some ridges appear to be symmetrical. The ridges are between 180 m and 1300 m apart, with a relative height between crests and swales of 3 to 12 m. The thickness of individual ridges (i.e. down to the bedrock) could not be observed clearly, however. Their composition includes bivalve, gastropod and arthropod (*Balanus* sp.) fragments forming cemented layers of calcarenite, calcirudite, coquina and pebbly coquina. Beach ridge crests crop out as calcrete, whereas the swales are composed of sandy soil. On satellite images, these are manifested as concentric lines parallel to the present shoreline, and in the field as alternating zones of contrasting materials and colors (Fig. 3 a, b).

4.2. Macromorphology

At all sites examined on terrace T_{II} a similar sequence of soil profiles exists (Fig. 4), consisting of a sandy layer overlying calcrete. The latter forms a well-defined pedogenic horizon with an A-Bw sequence in all profiles, except at Maitencillo which shows an A-Bw-Bt sequence (see Appendix for technical terms). Colors are dark brown (7.5YR 3/2, moist) for A-horizons, brown (7.5 YR 4/4, moist) for Bw-horizons and reddish brown (5YR 4/4, moist) for Bt-horizons. A- and Bw-horizons have a sub-angular blocky structure, whereas Bt-horizons display a columnar structure.

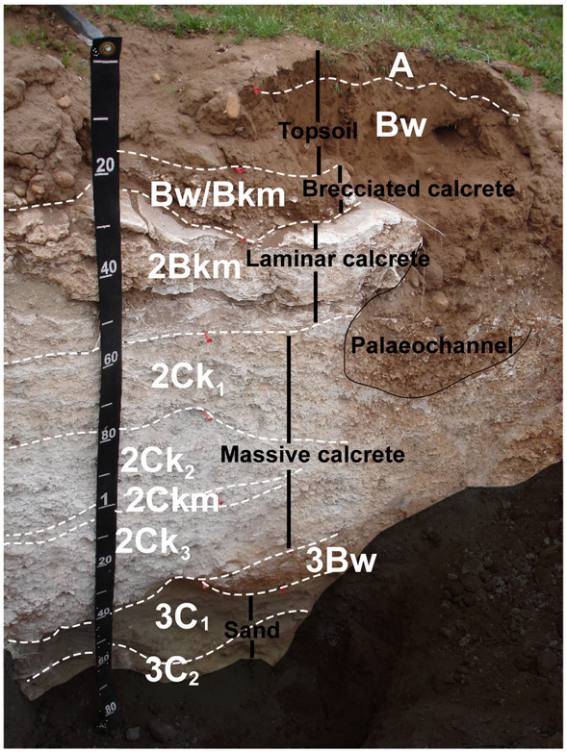

Fig. 5. La Montosa soil profile showing the main strata that compose the Tongoy Terrace T_{II} soil sequence; letters show soil horizons; note the palaeochannel that cuts the laminar and massive calcrete. Shaded area indicates removed soil material.

Machette (1985) recognized six stages of calcrete development, with specific diagnostic features for each stage. The calcrete of Tongoy can be divided into three parts: brecciated, laminar and massive calcrete, the upper part consisting of fragmented pieces of laminar calcrete mixed with the soil, followed by an almost continuous laminar calcrete with some micro-laminations. This layer corresponds to a petrocalcic horizon in soil taxonomy. Below this lies a sandy or sandy coquina layer cemented by massive carbonates, with a thickness between 40 and 60 cm. Within the massive calcrete, fossils are preserved that have a Pleistocene–Holocene distribution in the stratigraphic record (*Argopecten purpuratus, Concholepas concholepas, Crucibulum quiriquinae, Crepipatella dilatata, Incatella cingulata*), although some species also occur in Pliocene deposits (*Venus antiqua, Olivia peruviana, Balanus* sp.), with one reported only from the Pliocene, viz. *Chorus blainvillei* (DeVries, 1997; Guzmán et al., 2000). The existence of *C. blainvillei* within the Pleistocene beach ridge deposits can be explained by reworking of Pliocene deposits corresponding to the Coquimbo Formation.

Below this feature are a series of deposits ranging from loose sand to coarse shells and cemented sand. Laminar calcrete is always found where the profile developed over shell or fragmented shell deposits, which are an important calcium source. In localities where the substrate is richer in siliciclastic deposits, secondary calcium carbonate has been deposited in macroscopic rhizoliths or within soil cracks, the latter forming so-called honeycomb calcrete (Wright and Tucker, 1991) or interlacing carbonate lamination (Alonso et al., 2004)

Fragmented calcrete is also known as brecciated calcrete, and the processes which cause it include the displacive growth of carbonates, wetting and drying cycles, thermal expansion, and rhizobrecciation

Please cite this article as: Pfeiffer, M., et al., Preservation of beach ridges due to pedogenic calcrete development in the Tongoy palaeobay, North-Central Chile, Geomorphology (2011), doi:10.1016/j.geomorph.2011.05.012

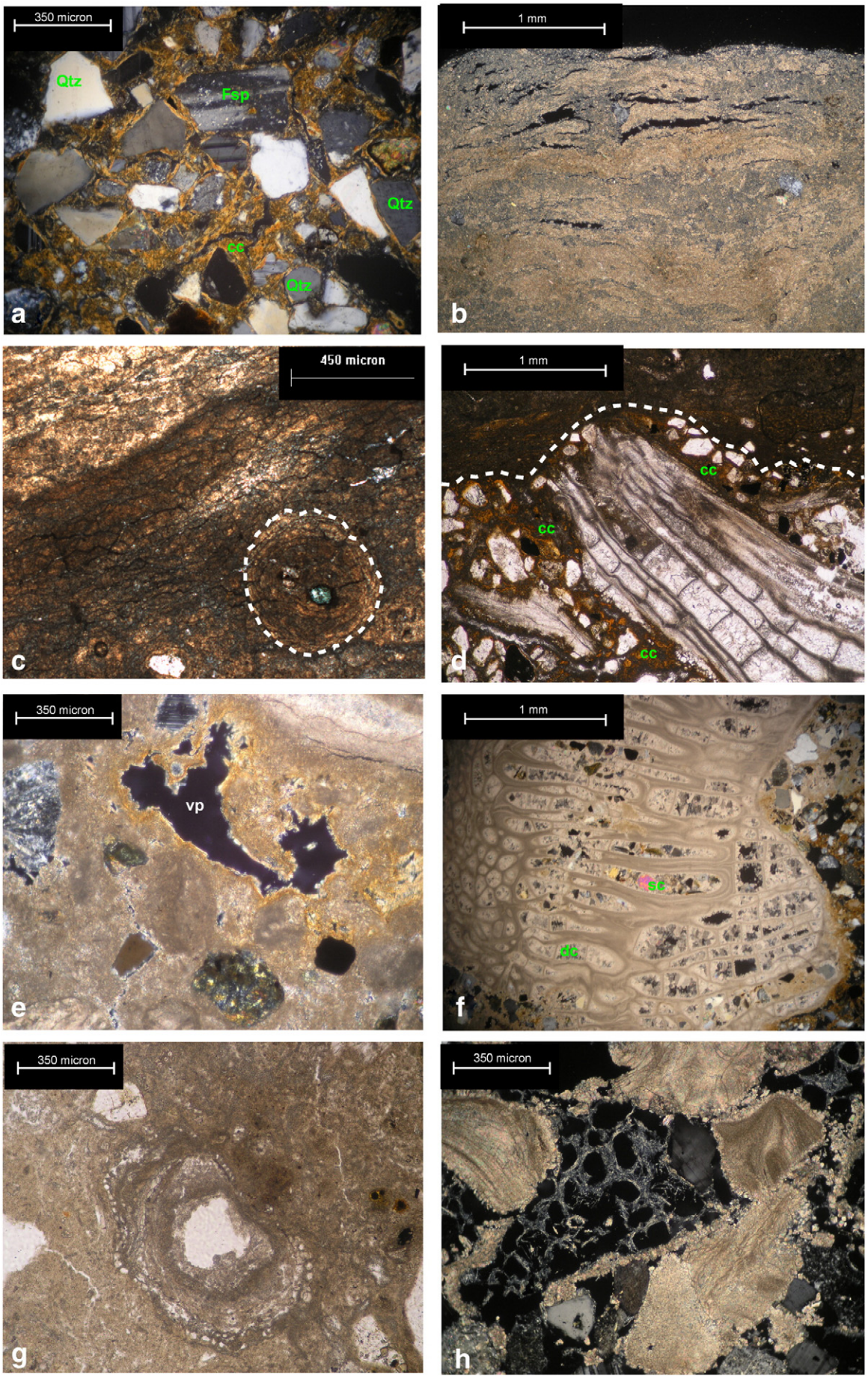

Please cite this article as: Pfeiffer, M., et al., Preservation of beach ridges due to pedogenic calcrete development in the Tongoy palaeobay, North-Central Chile, Geomorphology (2011), doi:10.1016/j.geomorph.2011.05.012

caused by the penetrative growth of roots (Klappa, 1980; Wright, 1994). In addition, antiformal structures resembling tepees are found, which may reflect the displacive growth of carbonates in other substrates (Watts, 1977). In some places between the cracks are layers with numerous pisoliths that contain quartz grains as nuclei, the matrix being similar to the topsoil, and roots being present within the cracks. Laminar calcretes also extend into vertical cracks, the laminae covering the crack walls like a continuous veneer, suggesting that carbonate precipitation occurs from vertical groundwater movement.

Massive calcretes can extend over more than one horizon, which are separated because of variations in hardness, clast size, color, and fossil composition.

Laminar and massive calcretes are locally cut by palaeochannels that contain well rounded clasts, suggesting a fluvial origin or marine reworking (Fig. 5). The palaeochannels also contain calcrete fragments, indicating that they eroded the calcrete and therefore formed subsequent to the latter.

4.3. Micro-morphology

The micromorphological features of the studied soil profiles can be classified in the same way as the macromorphological features (a sandy topsoil, laminar calcrete and massive calcrete). Both types of calcrete constitute a petrocalcic horizon, whose most important features are its hardness and resistance to erosion and its impermeability that restricts water infiltration.

4.3.1. Topsoil

The groundmass of the upper topsoil is dominated by quartz grains. Although these grains mostly have smooth rims, some of the borders are irregular, which is interpreted as resulting from weathering processes (Fig. 6a). Scarce shell fragments of sand size are also present. The micro-fabrics vary from chitonic to closed porphyric. The pores are composed of simple packing voids, channels, chambers, compound parting voids and planes. Fine material is clayey, pigmented with iron oxides; clay components have high interference colors and are oriented along sand grain surfaces and plane walls (porostriated and granostriated orientation) indicative of expansion and contraction processes (Fig. 6a). Some thin clay coatings covering pores and grains can also be observed below 20 cm (Fig. 6a). Fine ferruginous clay may result from the weathering of highly unstable grains such as biotite, volcanic fragments, and chert containing chlorite—we observed signs of patchy alteration in many rock fragments. Channel pores are associated with root growth. Excremental aggregates, which are signs of faunal activity, are also present, mostly associated with the roots and biogenic channels. Orthic Fe nodules of typic and alteromorphic types also occur, the latter referring to nodules whose internal fabrics are pseudomorphs after some material such as mineral fragments (Stoops, 2003).

4.3.2. Brecciated calcrete

This type of calcrete generally constitutes a transitional horizon in which the fractures of laminar calcretes are filled with the overlying soil. Thus, non-carbonate areas resemble the overlying material, being somewhat enriched in clay (open porphyric) with coatings covering grains. The contacts between both materials (carbonate and non-carbonate micro-areas) are sharp, but in some areas tiny carbonate fragments are incorporated within the matrix fill.

4.3.3. Laminar calcrete

Laminar carbonates have a thickness of about 15 cm, with four to five micro-laminae showing different micro-structrures. The crystal size is micritic to micro-sparitic, with mottling features that reflect patches with different crystal sizes. The upper micro-laminae exhibit an undulating pattern (Fig. 6b) with horizontal fractures, due probably to the displacive growth of carbonates. Siliciclastic grains are rare within the laminar calcrete, but vary from micro-laminae with less than 1% siliciclasts to micro-laminae with about 20% siliciclastic grains. The contacts between the micro-laminae are sharp, suggesting that each micro-lamina had formed during a different period. In the lower parts of the laminar calcrete, peloids and pisoliths appear (Fig. 6c). Bioclasts are present only in the lower parts of the laminar calcretes, most of them showing a micritic coating. Skeletal pores are also present, indicating the preferential degradation of bioclasts (Flessa and Brown, 1983). Within skeletal pores a drusy cement occurs that is associated with meteoric groundwater (Fig. 6d, f). Because no features of biogenic origin where found in the laminar calcrete, we classify them micro-morphologically as alpha calcretes (Wright, 1990).

There is a clear contact between the laminar calcrete and the underlying massive calcrete. Numerous bioclasts occur along the contact between both layers, some having a micritic coating (Fig. 6d). Dissolution of bioclasts is in some cases complete, forming a moldic porosity with clay coatings along the walls, and re-precipitated sparite cement in the center. Skeletal porosity with a drusy sparite cement dominates. Clay coatings covering vuggy pores and clastic grains are also present just below the border between laminar and massive calcrete. These clay coatings are oriented and show a high birefringence in the La Montosa and Alamito profiles (Fig. 6d) and are of impure clay pedofeatures in the Maitencillo profile, where they also covered with a micritic carbonate coating in vuggy voids (Fig. 6e). Cracks present along the contact between laminar and massive calcretes also contain columnar and needle sparitic cement.

4.3.4. Massive calcrete

Horizons forming part of the massive calcrete are classified at a microscopic level as wackestone, packstone and mudstone following Dunham (1962); and as packed biomicrite, sparse biomicrite, biopelmicrite, dismicrite and fossiliferous micrite after Folk (1962). The change in classification reflects differences in the dominance of carbonate components, although all horizons are predominantly calcareous.

Allochems are mainly bioclasts, with ooids, pisoliths, peloids and intraclasts also present. Bioclasts correspond mainly to fragmented parts of gastropods, bivalves and the arthropod *Balanus*. Foraminifera are also present in small quantities. The bioclasts show a selective solution of the shell fragments, thus forming a moldic porosity, which is filled by grains and sparitic cement in the form of drusy, needle and equant cement (Fig. 6h). The infilling of bioclast pores with clastic grains indicates that dissolution occurred before reworking of the material. The presence of drusy cement is associated with the meteoric vadose zone, columnar cement with mixed marine/meteoric water, and needle cement is linked to fungi. Bioclasts also present a micritic rim, sometimes with coatings that reflect a process similar to the formation of pisoliths. Ooids are a common feature and show a variety

Fig. 6. Micromorphology of soil profiles. (a) Oriented clay coatings (cc), quartz (Qtz) and feldspar (Fsp) grains with ondulating and platy pores in Maitencillo Bt_2 horizon. (b) Upper micritic microlaminae in Maitencillo laminar calcrete, 2Bkm horizon (for horizon nomenclature see Appendix). (c) Contact between second and third microlaminae, dotted line demarcates a pisolithic grain in the third lamina with a quartz nucleus, La Montosa 2Bkm horizon. (d) Dotted line shows contact between laminar (2Bkm) and massive calcrete ($2Ck_2$); the massive calcrete has thin clay cutans (cc) in pores and along clast rims, La Montosa profile. (e) Dirty clay cutans filling vuggy pore (vp) in micritic matrix in 2Ck1 horizon, Maitencillo. (f) Skeletal pores in *Balanus* sp. shell fragment due to selective solution of shells; drusy cement (dc) and siliciclastic grains (sc) fill the pores; $4C_1$ horizon, La Montosa. (g) Rhizolith transverse cut showing root cell petrification. (h) Equant circumgranular cement along bioclast borders and alveolar septal structure of needle cement; $2Ck_1$ horizon, Alamito.

Please cite this article as: Pfeiffer, M., et al., Preservation of beach ridges due to pedogenic calcrete development in the Tongoy palaeobay, North-Central Chile, Geomorphology (2011), doi:10.1016/j.geomorph.2011.05.012

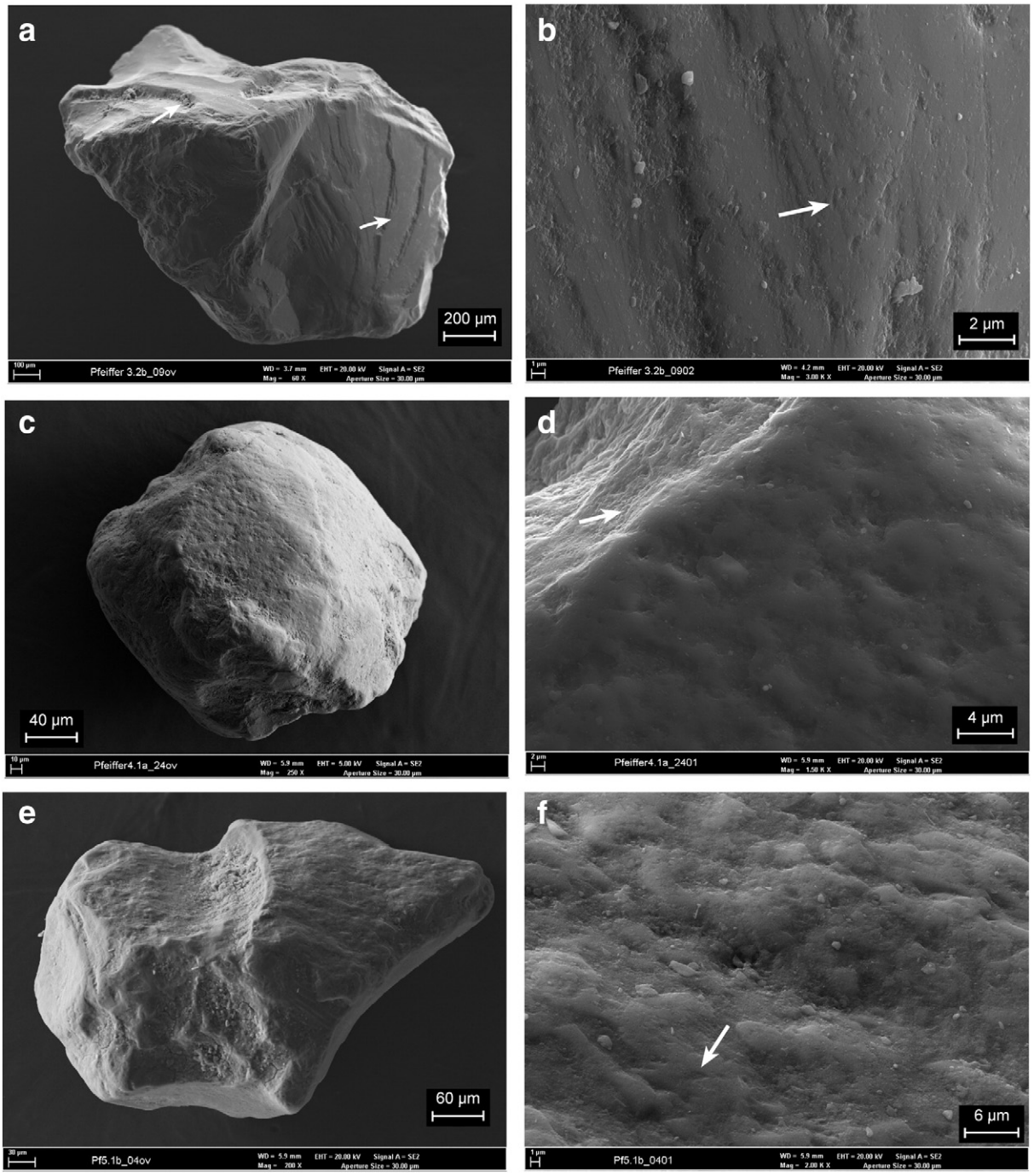

Fig. 7. SEM micro-photographs. (a) b-group grain showing the blocky, sub-angular shape of the oldest process (I). The shape and surface are dominated by V-shaped incisions, large fracture planes, edge grinding, step-like features, and crescent-shaped gouges (arrows). (b) Close-up of a large fracture plane reveals numerous, very small V-pits resulting from limited aeolian transport during the second process (II). (c) Rounded a-grain, completely encrusted by re-precipitated silica, and with partly well rounded edges. (d) More detailed view of a wind-abraded edge (process II; see arrow) and the smoothed, orange-peel texture that is densely pitted with V-marks. (e) Sub-angular to rounded b-grain, where large grooves, craters, and incision marks as well as the edges of process I became widely smoothed by aeolian abrasion (II), while finer details of the surface (f) became obscured by a rather thick silica veneer and some dissolution features possibly related to youngest chemical processes (III). Dissolution preferentially affects microcracks or dense sets of mechanical marks as seen in (f).

of nuclei consisting of siliciclastic grains, bioclasts or micritic intraclasts. The ooid coatings are very thin (50 µm), and the diameters of the ooids rarely exceed 2 mm. However, having the same characteristics as large coated grains (pisoliths), they can be considered as proto-pisoliths.

Micritic intraclasts with a grain size different from the micritic matrix are also present. This suggests different processes of micritization after and before reworking of the sediments.

Peloids are common in some horizons and appear frequently in agglomerations. The shape of the peloidal grains is well-rounded with both high and low sphericity. The peloid diameters range from 20 to 400 µm. Their origin could be the reworking of micritic material, as well as fecal.

Microscale features attributable to the activity of organisms are also present. These are rhizoliths, alveolar septal fabrics and needle calcite (attributed to fungal activity), blue green algae filaments and

Please cite this article as: Pfeiffer, M., et al., Preservation of beach ridges due to pedogenic calcrete development in the Tongoy palaeobay, North-Central Chile, Geomorphology (2011), doi:10.1016/j.geomorph.2011.05.012

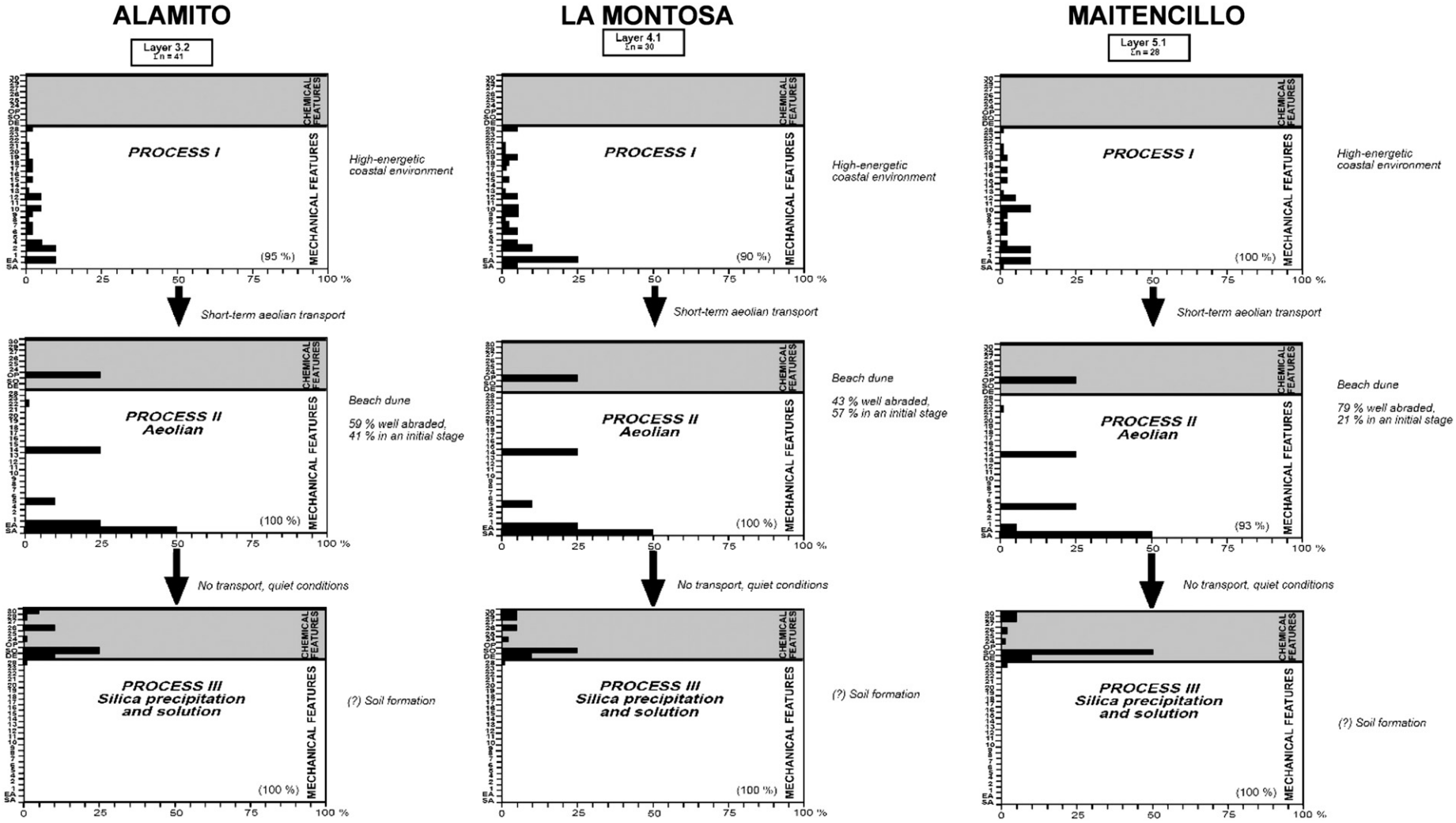

Fig. 8. Comparison of texture group patterns and visually estimated frequencies of single surface features. SA - surface abrasion; EA - edge abrasion; 1 - small blocks; 2 - large blocks; 4 - large uplifted plates; 5 - small uplifted plates; 6 - cracks on edges; 7 - linear grooves; 8 - curved grooves; 9 - deep grooves; 10 - craters; 11 - striation; 12 - V-shaped incisions; 13 - V-shaped pits of random and different sizes; 14 - V-shaped pits in series; 15 - crescent-shaped gouges; 16 - small conchoidal fractures; 17 - large conchoidal fractures; 18 - radial fractures; 20 - parallel steps; 21 - curved steps; 22 - ridges; 23 - sawtooth structures; DE - dissolution etching; SO - silica overgrowth; OP - orange peel texture; 24 - silica globules; 25 - crystal growth; 26 - solution pits; 27 - crystallographically oriented, etched pits; 28 - irregular cracks; 29 - polygonal cracks; 30 - etched grooves.

Please cite this article as: Pfeiffer, M., et al., Preservation of beach ridges due to pedogenic calcrete development in the Tongoy palaeobay, North-Central Chile, Geomorphology (2011), doi:10.1016/j.geomorph.2011.05.012

fecal peloids. Rhizoliths are observed only in microscale in the sampled profiles, whereas macroscopic rhizoliths where observed only in one outcrop in the Greditas area (eastward limit of terrace T_{II}), where the sediment is mainly siliciclastic in origin. The diameter of rhizoliths present in the studied profiles does not exceed 1 mm (Fig. 6g). Circumgranular equant cement, gypsum and halite are also present in the lower parts of the massive calcrete (Fig. 6h).

The main fabric elements of massive calcrete show a typical b-fabric, where the dominant processes are attributable to the existence and activities of macro- and micro- organisms (Wright, 1990).

4.4. Quartz grain surface analysis

To obtain further micromorphological information, three topsoil profiles were selected: Alamito, La Montosa, and Maitencillo. On average, the sampled material is of medium sand-size, which should guarantee a broad spectrum of mechanical erosion marks (Margolis and Krinsley, 1974; Krischev and Georgiev, 1981). Transport processes or other influences affecting the history of the grains cannot be defined by only a single mark or feature, but require a group of microfeatures, which should be typical for the same or a very similar

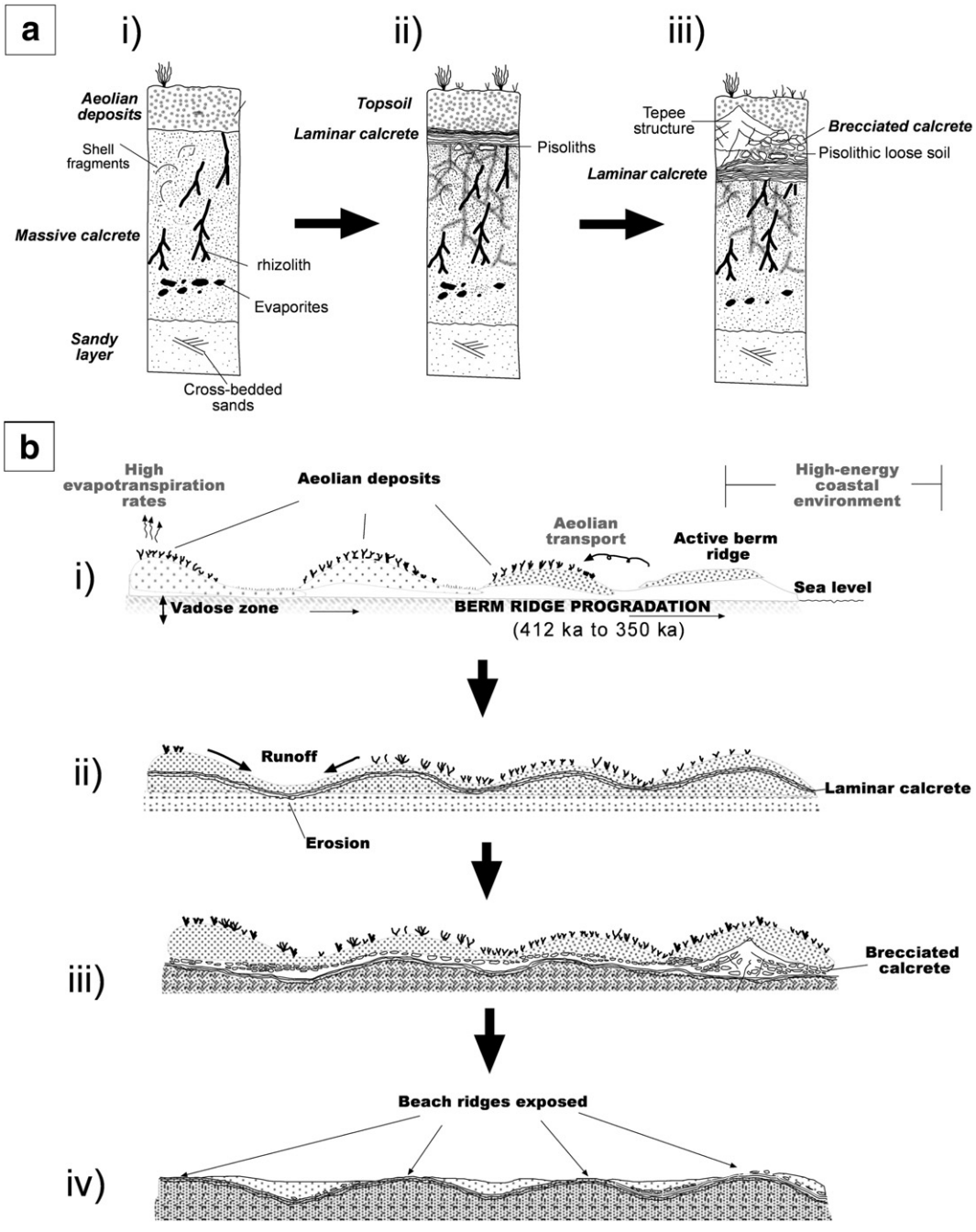

Fig. 9. Diagrams showing the Tongoy calcrete and landscape evolution. (a) Three main steps of calcrete evolution: i) Development of massive calcrete due mainly to biological processes of carbonate precipitation; ii) Development of laminar calcrete along the upper contact of the massive calcrete; iii) Development of brecciated calcrete due to fracturing and displacive growth of the laminar calcrete. (b) Geomorphological processes related to the Tongoy calcrete development: i) Beach ridge progradation left sandy shell fragments and a microtopography covered by aeolian deposits; ii) Water run-off produces erosion in depressions and the formation of a laminar calcrete because of ponded water; iii) Formation of brecciated calcrete and redistribution of deposits; iv) Beach ridge crests are preserved by laminar and brecciated calcrete, whereas swales contain topsoil as shown in Fig. 3b.

Please cite this article as: Pfeiffer, M., et al., Preservation of beach ridges due to pedogenic calcrete development in the Tongoy palaeobay, North-Central Chile, Geomorphology (2011), doi:10.1016/j.geomorph.2011.05.012

type of motion in a certain transport medium. These are the so-called microtexture groups (Krinsley and Donahue, 1968; Higgs, 1979; Bull, 1981; Mahaney, 2002).

Under the SEM, the (a)- and (b)-parts of the divided samples show additional differences not noted under the stereomicroscope. The (a)-subsample grains are slightly larger on average (≥500 μm), tend to be sub-rounded, and exhibit more intensive aeolian abrasion (Fig. 7c) compared to the more angular and smaller (b)-subsample grains (<500 μm; Fig. 7a, e). The majority of (a)-grains, especially those that are semi-transparent to opaque, however, turned out to be feldspar. Since the hardness, cleavage, and other mechanical properties of quartz and feldspar differ from each other, feldspar grains were eliminated, which inevitably reduced the number of analyzed grains. The resulting data, however, prove that both (a)- and (b)-quartz grains are characterized by the same three micro-texture groups, thus allowing a combined analysis. The remaining number of grains still complies with that required for statistical confidence ($n \geq 30$; Trewin, 1988). Plotted on micro-texture frequency diagrams (Fig. 8), the patterns of the studied samples show a high resemblance to each other. Slight variations in the frequencies of single features probably reflect a random spread of data.

Each of the three successive micro-texture groups is assumed to represent a single transport process. Group I is represented by the oldest erosion marks, such as V-shaped marks and incisions, as well as crescent-shaped marks of different sizes that are randomly distributed (Fig. 7a). Fracture features dominate, causing a rather blocky or shard-like surface (conchoidal and step-like features) and relatively high relief. Edge abrasion rarely results in rounding. Together with their transparency and often triangular to wedge shape, which are shown by roughly half of the grains, a short-lived transport process in a high energy environment can be concluded (Fig. 8). These features may be associated with transport by periodic swashing on a beach or terrestrial run-off. In particular, grains from Alamito show adherent fibrous plant relics that indicate the illuviation of terrestrial material. The adherent particles, however, cannot be defined as a distinct feature of process I; they could also be related to a later stage, when vegetation colonized the sand layer as well as the underlying calcrete. Some grains also show evidence of longer transport distances in water, where rounded edges are associated with some degree of surface abrasion, and which are clearly not due to the subsequent aeolian abrasion.

Group II (Fig. 8) reflects the dominant process, showing well defined aeolian transport features (Fig. 7d, f). Here, the rather incomplete abrasion of the grains (Fig. 8; Fig. 7b) before incorporation into the sediments seems to be typical for marine beach dunes. As more than 90 to 100% of the wind-abraded grains bear the preceding micro-texture group, Group II only reflects reworking of the formerly deposited sediment.

Group III represents a chemical surface process that may be due to soil formation. Silica precipitation on top of the orange-peel texture that formed during aeolian reworking indicates periods of quiescence. It mainly occurs as a veneer- or crust-like overgrowth (Fig. 7e, f).

5. Interpretation

We propose that the formation of calcrete at Tongoy resulted from a sequence of processes (Fig. 9), starting with the reworking of calcareous deposits belonging to the Coquimbo Formation during Pleistocene marine transgressions. Terrace abrasion during the sea-level highstand was coupled with active biogenic shell production on the adjacent shelf. This process produced mixed material of older reworked sediments and new biogenic clasts that were deposited in

Table 1
Chemical properties of studied profiles (data from Las Tortolas profile are taken from Aburto et al., 2008). Abbreviations: BD, bulk density; EC, electrical conductivity; OM, organic matter; CEC, cation exchange capacity; ESP, sodium exchange percentage; nd, not determined.

Profile	Lab code	Horizon	Depth (cm)	BD ($kg\ m^{-3}$)	EC dS m^{-1}	pH (H_2O) (1:25)	OM%	HCO_3	Cl	SO_4	CEC	Na	K	Ca	Mg	ESP%	Ca/Na
								$cmol + kg^{-1}$									
Tortolas	08N02981	A	0–8	nd	0.95	8.2	1.03	4.40	3.40	0.60	4.80	0.10	0.60	20.20	1.10	0.45	202.00
	08N02982	Bw_1	8–28	1.67	1.10	8.0	0.57	2.30	9.30	0.50	5.30	0.40	0.30	7.80	1.00	4.21	19.50
	08N02983	Bw_2	28–39	nd	1.03	7.8	0.60	3.70	5.20	1.20	15.60	1.20	0.40	18.40	3.70	5.06	15.33
	08N02984	Bw/Bkm	39–56	1.53	10.78	8.0	0.83	1.70	107.00	10.90	26.50	12.90	0.60	35.80	10.30	21.64	2.78
	08N02985	2Bkm	56–85	nd	22.90	8.0	14.67	1.00	245.80	21.70	3.40	15.50	0.20	48.90	3.40	22.79	3.15
	08N02986	$2Ckm_1$	85–117	nd	65.00	8.4	11.84	1.00	874.00	63.60	4.00	39.30	0.10	45.90	3.10	44.46	1.17
Alamito	9710	A	0–1	1.49	0.51	7.50	1.35	3.50	0.04	0.67	12.00	0.75	5.07	7.28	0.66	5.45	9.71
	9711	Bw	1–5	1.61	0.63	8.00	1.14	3.30	0.15	0.38	12.00	0.87	2.70	2.47	0.58	13.14	2.84
	9712	Bw/Bkm	5–23	1.56	14.85	8.92	nd	2.20	0.85	2.55	15.80	2.09	0.59	13.95	1.17	11.74	6.67
	9713	2Bkm	23–33	1.78	0.81	8.85	nd	1.50	0.38	0.38	10.20	0.77	0.16	15.33	1.09	4.44	19.91
	9714	$2Ckm_1$	33–58	1.62	0.32	9.05	nd	1.40	0.00	0.77	9.30	4.13	0.17	11.09	0.82	25.48	2.69
	9715	2Ck	58–70	1.54	0.44	9.02	nd	2.20	0.08	0.31	8.10	4.55	0.15	10.49	0.83	28.40	2.31
	9716	A	0–5	1.68	0.62	7.00	1.98	3.40	0.00	0.83	14.40	0.75	8.00	5.78	0.83	4.88	7.71
	9717	Bw	5–23	1.71	0.61	7.00	0.90	1.50	0.00	0.61	14.70	0.87	6.24	5.53	0.92	6.42	6.36
	9718	Bw/Bkm	23–36	1.58	17.2	8.00	1.10	2.50	0.12	0.22	16.90	2.09	5.71	3.60	1.00	16.85	1.72
	9719	2Bkm	36–56	nd	7.96	8.95	nd	1.50	0.28	1.83	14.80	0.77	1.96	13.00	1.00	4.60	16.88
La Montosa	9720	$2Ck_1$	56–77	1.98	5.20	8.40	nd	1.60	0.26	1.05	11.40	1.88	1.26	12.00	1.00	11.65	6.38
	9721	$2Ck_2$	77–101	2.15	11.7	8.95	nd	1.60	0.16	1.89	4.30	37.51	0.42	3.39	0.17	90.41	0.09
	9722	2Ckm	101–103	1.90	83.7	8.85	nd	2.00	0.14	0.32	7.80	37.54	0.42	2.07	0.05	93.66	0.06
	9723	$2Ck_3$	103–136	1.71	29.8	9.00	nd	1.80	0.06	0.4	8.96	37.61	5.07	2.13	0.05	83.84	0.06
	9724	3Bw	136–156	1.69	47.7	8.48	nd	2.00	0.28	6.91	11.28	38.88	2.70	2.48	0.10	88.04	0.06
	9725	$3C_1$	156–170	1.87	6.45	8.72	nd	3.80	0.06	0.28	8.83	37.18	2.70	11.05	0.73	71.97	0.30
	9726	$3C_2$	170–190	1.80	24.9	8.62	nd	1.50	0.10	0.97	5.14	37.53	0.16	1.01	0.07	96.80	0.03
	9727	A	0–4	1.50	62.1	7.25	1.00	3.50	0.05	0.41	5.27	37.18	0.17	0.31	0.05	98.59	0.01
	9728	Bw	4–12	1.61	12.8	7.00	0.90	3.30	0.00	0.54	8.32	37.63	0.15	0.43	0.08	98.28	0.01
	9729	Bt_1	12–26	1.78	20.6	6.40	0.59	1.50	4.22	4.24	7.66	70.40	6.24	0.55	0.34	90.80	0.01
	9730	Bt_2	26–47	1.82	61.0	7.00	0.68	1.40	4.99	8.38	10.52	70.76	5.71	3.62	0.53	87.77	0.05
Maitencillo	9731	Bt_2/2Bkm	47–58	1.87	48.5	8.10	0.49	2.20	21.21	32.90	11.15	112.96	1.96	2.55	0.49	95.76	0.02
	9732	2Bkm	58–67	nd	43.8	8.20	nd	1.38	13.09	39.90	7.64	81.85	1.96	2.64	0.19	94.47	0.03
	9733	$2Ck_1$	67–82	1.82	18.3	8.50	nd	1.00	9.43	54.20	4.30	77.36	1.96	2.37	0.17	94.50	0.03
	9734	$2Ck_2$	82–106	1.88	8.20	8.50	nd	2.20	10.10	57.00	3.93	75.18	1.96	5.56	0.30	90.58	0.07
	9735	$2Ck_3$	106–123	1.77	4.88	8.22	nd	1.00	28.46	41.15	5.98	86.20	2.0	2.88	0.31	94.36	0.03
	9736	$2Ck_4$	123–136	1.83	20.6	9.12	nd	2.20	5.76	43.24	6.02	65.47	1.26	1.85	0.13	95.28	0.03

Please cite this article as: Pfeiffer, M., et al., Preservation of beach ridges due to pedogenic calcrete development in the Tongoy palaeobay, North-Central Chile, Geomorphology (2011), doi:10.1016/j.geomorph.2011.05.012

prominent berms. Sea-level retreat after the MIS 11 highstand, possibly influenced by tectonic pulses, produced a series of beach ridges representing these ancient shorelines. In the early stages of development, preferential dissolution of aragonitic shell fragments would have released significant amounts of Ca^{+2} into the environment. This would have reprecipitated in the vadose zone as circumgranular equant calcite cement while this zone was dominated by mixed marine/meteoric waters. Halite and gypsum are highly soluble salts and their presence in the lower parts of the massive calcrete could be due to high evaporation rates in a shoreline environment or to the translocation of these salts to their equilibrium depth. This process could have been more intensive during certain periods or at specific localities on the progradation surface, which would explain the higher amounts of Cl^- and SO_4^{2-} in the Maitencillo profiles (Table 1). The presence of columnar cement is also associated with mixed marine-meteoric environments (Adams et al., 1984). Needle cement, on the other hand, is attributed by some authors to the supersaturation of calcium carbonate, although most authors associate it with fungi hiphae (Wright, 1994).

During these initial stages of development the sediments could not resist the penetration of roots, so that the latter played an important role in calcite precipitation during wetting-drying cycles. The diameter of rhizoliths present in the studied profiles does not exceed 1 mm (Fig. 6g), which suggests either a very short period of plant colonization, or a vegetation cover composed mainly of herbaceous species. Rhizoliths form due to the accumulation of pedogenic carbonates in the radical zone. If they develop while the plant is still alive, well-preserved root cells are left behind as shown in Fig. 6g (Wright and Tucker, 1991).

An important association with mycorhize can be interpreted from the alveolar septal structure and the large amount of needle calcite. Alveolar septal structures are common in massive calcrete, occupying mostly channels and vuggy pores, but may also be present in other types of pores (Fig. 6h). These structures are related to mycelia bundles, which occur in association with root tubules due to mycorrhizal activity (Wright and Wilson, 1987). Needle-fiber calcite is the most common cement in pores of massive calcrete and is closely related to alveolar septal structures, of which it forms the main component. These are thought to originate from fungal biomineralization (Callot et al., 1985; Verrecchia and Verrechia, 1994; Verrechia and Dumont, 1996; Bezce-Deak et al., 1997; Loisy et al., 1999). Plant association with mycorrhizal fungi in this type of soil has an important effect on improving plant growth under drought conditions (Navarro-Fernández et al., 2011), which could explain the high density of alveolar septal structures.

The presence of peloids in the Tongoy calcrete may be interpreted as reworked fragments of a micritic matrix (Freytet and Plaziat, 1982; Sarkar, 1988; Platt, 1989; Wright et al., 1990). However, they may also reflect the presence of organisms that contributed to the formation of a beta-fabric calcrete. The formation of beta calcrete is associated with a semi-arid to humid environment with an extensive vegetation cover in parent materials rich in carbonates (Wright, 1990; Wright and Tucker, 1991).

Continued cementation of calcite in the pore spaces caused a hardening of the calcrete and a gradual decrease in permeability. The presence of a groundwater table and associated vadose zone during humid periods also contributed to the precipitation of sparite cement, forming a drusy texture that is common in the skeletal pores of bioclasts. The calcrete is overlain by a leached and weathered Bw horizon, suggesting that part of the carbonate cementation may have been caused by illuviation of carbonates from overlying strata. This process must have occurred before the illuviation of clay. Coatings and hipocoatings of carbonates filling pores reflect recrystallization and illuviation due to pedogenic development subsequent to previous processes such as the formation of channel pores resulting from root growth.

Pisoliths (or pisoids) in the Tongoy T_{II} profiles occur in the upper parts of the massive calcrete and many of them have asymmetrical coatings, suggesting that they formed in situ when the lower substrate was indurated. They show preferential growth on the lower surface (pendant coatings), which indicate that they remained immobile within the vadose zone (Hay and Reeder, 1978). The presence of pisoliths is associated with mature calcrete profiles following hardpan formation (Wright and Tucker, 1991). The most abundant layers of pisoliths are just below the laminar calcrete, reflecting a stage where the bottom layer had become less permeable.

Below the soil profile at La Montosa is sand devoid of carbonates and showing grain micro-structures without any sign of clay illuviation. This indicates that pedogenic processes occurred up to a limited depth, and that calcrete formation at Tongoy was mostly, if not entirely, due to pedogenic processes.

Clay films occurring in the upper part of massive calcrete along the contact with laminar calcrete have several implications. In the first place, the sand layer must have been weathered sufficiently to provide silica for clay formation and translocation. Secondly, the rainfall increased sufficiently for clay illuviation to occur. Thirdly, the fact that illuvial pedofeatures are separated from the upper elluvial horizons implies that these would have formed at an earlier stage than the formation of laminar calcrete, a process also described for Morocco calcretes by Bronger and Sedov (1997) and for the Yucatán Peninsula calcretes by Cabadas et al. (2010). Maitencillo clay coatings are impure, which is explained by Pal et al. (1994) as an impairment of the parallel orientation of the clay platelets induced by the disruption of both clay- and silt-size layer silicates in a Na-rich environment. These authors propose that a high amount of sodium causes the precipitation of soluble Ca^{2+} ions as calcium carbonate, preventing the flocculation of Ca^{2+}. This would coincide with the high amount of ESP (Exchangeable Sodium Percentage) of this profile. On the other hand, clay coatings of the younger profiles are well-oriented with a high birefringence, whereas the ESP in the upper horizons is considerably lower in comparison with that of the Maitencillo profile (Table 1). Clay coatings in these profiles were emplaced before carbonate precipitation in the pore space between the grains, interpreted by some authors as reflecting a climate change from wet to dry conditions (Allen and Goss, 1974; El-Tezhani et al., 1984; Reheis, 1987). According to Kuenen and Perdok (1962), silica solubility is enhanced by the enrichment of alkaline fluids due to the cyclic variation of evaporation and condensation under arid conditions. The underlying carbonaceous bedrock may have provided the necessary alkalis. Subsequently, within this continuous cycle, silica will be re-precipitated (Krinsley and Doornkamp, 1973).

SEM analysis on quartz grains shows peeling and cracks, some having a polygonal pattern that indicates spells of aridity during the palaeosoil formation. It is also important to mention that the presence of brecciated calcretes implies the previous formation of laminar calcrete so that the time span between the formation of massive calcrete and clay illuviation could be significant.

The presence of topsoil of aeolian origin that was more porous than the underlying massive calcrete, may have allowed the formation of a ponded water table. This is supported by Fe nodules in the Bw horizon, which are related to redoximorphic processes. The existence of a ponded water table during humid periods favored the formation of laminar calcrete along the contact between the layers because of the differences in CO_2 partial pressure (pCO_2) between both layers. The relatively higher moisture content in the ponded water limited gas diffusion, so that the pCO_2 increased but decreased near the contact with the massive calcrete. This would have allowed the precipitation of laminar calcrete along the contact between both strata.

The formation of laminar calcrete represents an advanced stage in Machette's (1985) stages of calcrete development. This agrees with our observations of calcrete development, which included the development of a dense micro-fabric with displacive precipitation of carbonates and the formation of complex cracks.

Please cite this article as: Pfeiffer, M., et al., Preservation of beach ridges due to pedogenic calcrete development in the Tongoy palaeobay, North-Central Chile, Geomorphology (2011), doi:10.1016/j.geomorph.2011.05.012

The last stage in the development of calcrete included fracturing of the laminar calcrete to produce brecciated calcrete. This took place by displacive growth, as indicated by the formation of tepee structures, and root growth that facilitated its infilling with topsoil material. Subsequently, pisolithic layers developed and meteoric water moved into the cracks, allowing the formation of a new laminar calcrete below the brecciated calcrete.

Subsequent to the formation of this petrocalcic horizon erosion took place, as indicated by numerous palaeochannels cutting into it (Fig. 5). Nevertheless, the existence of a petrocalcic horizon with a great resistance to mechanical and chemical weathering below the topsoil accentuated the ridge–swale landscape by forming a physical barrier to water infiltration. On the beach ridges themselves, little erosion took place as the surface water flowed laterally from here towards the swales. However, the accumulation of rainwater within the swales caused an increase in the water volume and consequently the flow velocity, so that the erosion rate would have been higher here than on the neighboring ridges. This is demonstrated by the drainage pattern of the tributaries on the T_{II}-terrace, which are parallel to the beach ridges as well as the shoreline (Fig. 2 a). The presence of vertical fractures within the calcrete could have favored the vertical incision and formation of gullies within the swales.

Precipitation is an important cause of erosion in the area (Owen et al., 2011), depending as in many arid climates on rare, extreme events (Coppus and Imeson, 2002). Such events in the study area are associated with the El Niño-Southern Oscillation cycle (Vargas et al., 2006), that commenced along the Southeastern Pacific coastline at least 5500 years ago (Rodbell et al., 1999; Jenny et al., 2002; Vargas et al., 2006). However, it may have started even before the end of the Pliocene according to Ravelo et al. (2004). Erosion rates in the area are about 40 m Ma^{-1} (Owen et al., 2011) and may have been higher during the wetter periods of the late Pleistocene and Holocene (Veit, 1993, 1996; Grosjean et al., 1997; Lamy et al., 1998; Maldonado and Villagrán, 2002, 2006).

6. Conclusions

In the Tongoy palaeobay, a beach–ridge topography was left on the marine T_{II}-terrace during marine regression and seaward progradation after the MIS 11 highstand (Fig. 9). These beach ridges are composed mainly of marine shell deposits that formed an important source of calcium carbonate, which allowed the formation of an indurated, erosion-resistant pedogenic calcrete that reached the VI stage of development according to Machette (1985). Calcrete development was driven first by biogenic agents and then by inorganic processes, forming massive and laminar calcretes, respectively. The latter suffered brecciation processes due to displacive growth and root action. Over the calcrete an aeolian sand cover was deposited that also underwent pedogenic processes. The calcretes preserved the micro-relief left by the post-MIS 11 seaward progradation due to their resistance to mechanical and chemical erosion. Drainage in the area is therefore characterized by gullies within the shore-parallel swales, forming a sub-parallel, trellis drainage pattern.

Acknowledgments

The first author is grateful to CONICYT and the Departamento de Postgrado y Postítulo, Universidad de Chile, for a fellowship that supported this study. We appreciate the help of Jaime Diaz and Eligio Jimenez for thin section preparation, Sven Nielsen for identifying the macrofossils within the calcrete and underlying soil, and Marysol Aravena for soil chemical analysis. Our special thanks go to Jose Padarian who actively participated in two field expeditions. The original manuscript benefited greatly from the suggestions of two anonymous reviewers.

Appendix A. Soil horizon terminology used in the study; descriptions are according to Schoenberger et al. (2002)

Horizon nomenclature	
Horizon	Criteria
A	Mineral soil, formed normally at surface, with little remnant rock structure.
B	Mineral soil, typically formed below A, with little or no rock structure; and one or more of the following: 1) Illuvial accumulation of silicate clay, Fe, Al, humus, carbonate, gypsum, silica or salt more soluble than gypsum (one or more) 2) Removal of carbonates, gypsum or more soluble salts; 3) Residual accumulation of sequioxides; 4) Sesquioxide coatings; 5) Alterations that form silicate clays or liberate oxides and forms pedogenic structure.
C	Mineral soil, soft bedrock; layer little affected by pedogenesis and lack properties of O, A, E, or B horizons. May or may not be related to the parent material.
B/C	Discrete, intermingled bodies of two horizons; majority of horizon is B material
Horizon suffixes	
Suffix	Criteria
k	Pedogenic accumulation of carbonates
m	Strong pedogenic cementation or induration (>90% cemented, even if fractured); physically root restrictive; cement type can be indicated using letter combinations; e.g., km - carbonates cementation.
t	Illuvial accumulation of silicate clays (clayskins, lamellae, or clay bridging in some part of the horizon)
w	Incipient color or pedogenic structure development; minimal illuvial accumulations (excluded from use with transition horizons)
Horizon prefixes	
	Horizon prefixes indicate a lithological discontinuity, for instance a 2B horizon after a B horizon indicate different provenance of the material or different moments of deposition.

References

Aburto, F., Hernández, C., Pfeiffer, M., Casanova, M., Luzio, W., 2008. Northern field—guide. The International Conference and Field Workshop on Soil Classification. Soil: a Work of Art of the Nature. Universidad de Chile, Santiago.

Adams, A.E., Mackenzie, W.S., Guilford, C., 1984. Atlas of Sedimentary Rocks under the Microscope. Longman, Wiley, New York-London.

Allen, B.L., Goss, D.W., 1974. Micromorphology of paleosols from the semiarid southern high plains of Texas. In: Rutherford, G.K. (Ed.), Soil Microscopy: Proceedings of the 4th International Working Meeting on Soil Micromophology. Limestone Press, Kingston, Ontario, pp. 511–525.

Alonso, P., Dorronsoro, C., Egido, J.A., 2004. Carbonatation in palaeosols formed on terraces of the Tormes River basin (Salamanca, Spain). Geoderma 118, 261–276.

Alonso-Zarza, A.M., Wright, V.P., 2010. Calcretes. In: Alonso-Zarza, A.M., Tanner, L.H. (Eds.), Carbonates in Continental Settings: Facies, Environments and Processes: Developments in Sedimentology, 61. Elsevier, Amsterdam, pp. 225–268.

Amiotti, N., Blanco, M.C., Sanchez, L.F., 2001. Complex pedogenesis related to differential aeolian sedimentation in microenvironments of the southern part of the semiarid region of Argentina. Catena 43, 137–156.

Armijo, R., Thiele, R., 1990. Active faulting in northern Chile: ramp stacking and lateral decoupling along a subduction plate boundary? Earth and Planetary Science Letters 98, 40–61.

Augustinus, P.G.E.F., 1989. Cheniers and chenier plains: a general introduction. Marine Geology 90, 219–229.

Benado, D.E., 2000. Estructuras y estratigrafía básica de terrazas marinas en sector costero de Altos de Talinay y Bahía Tongoy: implicancia neotectónica. Memoria Geología, Universidad de Chile, Santiago, Chile.

Bezce-Deak, J., Langhor, R., Verrechia, Ep.P., 1997. Small secondary scale $CaCO_3$ accumulation in selected sections of the European loess belt. Morphological forms and potential for paleoenvironmental reconstruction. Geoderma 76, 221–252.

Birkeland, P.W., 1999. Soils and Geomorphology. Oxford Univ. Press, New York.

Blanco, M.C., Stoops, G., 2007. Genesis of pedons with discontinuous argillic horizons in the Holocene loess mantle of the southern Pampean landscape, Argentina. Journal of South American Earth Sciences 23, 30–45.

Bookhagen, B., Echtler, H.P., Melnick, D., Strecker, M.R., Spencer, J.Q.G., 2006. Using uplifted Holocene beach berms for paleosismic analysis on the Santa María Island, south-central Chile. Geophysical Research Letters 33, L15302.

Please cite this article as: Pfeiffer, M., et al., Preservation of beach ridges due to pedogenic calcrete development in the Tongoy palaeobay, North-Central Chile, Geomorphology (2011), doi:10.1016/j.geomorph.2011.05.012

Brock, A.L., Buck, B.J., 2009. Polygenetic development of the Mormon Mesa, NV petrocalcic horizons: geomorphic and paleoenvironmental interpretations. Catena 77, 65–75.

Bronger, A., Sedov, S.N., 1997. Origin and redistribution of pedogenic clay in terrae rossae from Quaternary calcarenites in coastal Morocco. In: Shoba, S., Gerasimova, M., Miedema, R. (Eds.), Soil Micromorphology: Studies on Soil Diversity, Diagnosis Dynamics. Moscow-Wageningen, pp. 59–66.

Brüggen, J., 1950. Fundamentos de la Geología de Chile. Instituto Geográfico Militar, Santiago de Chile.

Bull, P.A., 1981. Environmental reconstruction by scanning electron microscopy. Progress in Physical Geography 5, 368–397.

Bullock, P., Fedoroff, N., Jongerius, A., Stoops, G., Tursina, T., Babel, U., 1985. Handbook for Soil Thin Section Description. Waine Research Publications, Wolverhampton, U.K.

Cabadas, H., Solleiro-Rebolledo, E., Sedov, S., Pi, T., Alcalá, J.R., 2010. The complex genesis of red soils in Peninsula Yucatan, Mexico: mineralogical, micromorphological and geochemical proxies. Eurasian Soil Sciences 13, 1439–1457.

Callot, G., Guyon, A., Mousain, D., 1985. Inter-relations entre aguilles de calcite et hyphes mycelliens. Agronomie 5, 209–216.

Chávez, C., 1967. Terrazas de abrasión. In: Thomas, H. (Ed.), Instituto de Investigaciones Geológicas, Boletín, 324. Geología de la Hoja Ovalle, Provincia de Coquimbo, pp. 137–140.

CIREN, 1990. Atlas Agroclimático de Chile, Regiones IV a IX. Ministerio de Agricultura de Chile. Centro de Información sobre Recursos Naturales, Publicacion, Santiago, Chile. Nº 87.

Coppus, R., Imeson, A.C., 2002. Extreme events controlling erosion and sediment transport in a semi-arid sub-Andean valley. Earth Surface Processes and Landforms 27, 207–236.

Darwin, C., 1846. Geological Observations on South America. Smith, Elder and Co, London.

DeVries, T.J., 1997. A review of the genus *Chorus* Gray, 1847 (Gastropoda: Muricidae) from western South America. Tulane Studies in Geology and Paleontology 30, 125–145.

Domeyko, I., 1848. Mémoire sur le terrain et les lignes d'ancien niveau de l'Océan du sud, aux environs de Coquimbo (Chili). Annales des Mines 14, 153–162.

Dunham, R.J., 1962. Classification of carbonate rocks according to depositional texture. In: Ham, W.E. (Ed.), Classification of Carbonate Rocks, 11. American Association of Petroleum Geologists Memoir, pp. 108–121.

Dunne, T., 1978. Field studies of hillslope flow processes. In: Kirkby, M.J. (Ed.), Hillslope Hydrology. John Wiley and Sons, New York, pp. 227–294.

El-Tezhani, M.S., Gradusov, B.P., Rubilina, N.Ye., Chizikova, N.P., 1984. Chemical and mineral composition of the finely dispersed component and microstructure of some soils in Sudan. Soviet Soil Science 16, 75–81.

Emparan, C., Pineda, G., 2006. Geologia del Area Andacollo-Puerto Aldea, Región de Coquimbo. Escala 1:100.000. Servicio Nacional de Geología y Mineria, Chile.

Eppes, M.C., McFadden, L.D., Matti, J., Powell, R., 2002. Influence of soil development on the geomorphic evolution of landscapes: an example from the Transverse Ranges of California. Geology 30, 195–198.

Flessa, K.W., Brown, T.J., 1983. Selective solution of macroinvertebrate calcareous hard parts: a laboratory study. Lethaia 16, 193–205.

Folk, R.L., 1962. Spectral subdivision of limestone types. In: Ham, W.E. (Ed.), Classification of Carbonate Rocks, 11. American Association of Petroleum Geologists Memoir, pp. 62–84.

Freytet, P., Plaziat, J.C., 1982. Continental carbonate sedimentation and pedogenesis—Late Cretaceous and Early Tertiary of southern France. Contributions to Sedimentology 12. Schweizerbart'sche Verlag, Stuttgart.

Gajardo, R., 1994. La Vegetación Natural de Chile. Clasificación y Distribución Geográfica. Editorial Universitaria, Santiago, Chile.

Gallala, W., Gaied, M.E., Essefi, E., Montacer, M., 2010. Pleistocene calcretes from eastern Tunisia: the stratigraphy, the microstructure and the environmental significance. Journal of African Earth Sciences 58, 445–456.

Gile, L.H., Petersen, F.F., Grossman, R.B., 1966. Morphological and genetic sequence of carbonate accumulation in desert soils. Soil Science 101, 347–360.

Grosjean, M., Valero-Garcés, B.L., Geyh, M.A., Messerli, B., Schotterer, U., Schreier, H., Kelts, K., 1997. Mid and late-Holocene limnogeology of Laguna del Negro Francisco, northern Chile, and its palaeoclimatic implications. The Holocene 7, 151–159.

Guzmán, N., Marquardt, C., Ortlieb, L., Frassinetti, D., 2000. La malacofauna neógena y cuaternaria del área de Caldera (27º–28ºS): especies y rangos bioestratigraficos. Actas del IX Congreso Geológico Chileno, Puerto Varas, Vol. 1, pp. 476–481.

Hay, R.L., Reeder, R.J., 1978. Calcretes of Olduvai Gorge and the Ndolanya beds of northern Tanzania. Sedimentology 25, 649–673.

Heinze, B., 2003. Active Intraplate Faulting in the Forearc of North Central Chile (30°S): Implications from Neotectonic Field Studies, GPS Data, and Elastic Dislocation Modeling. Scientific Technical Report. Geoforschungszentrum, Potsdam.

Herm, D., 1969. Marines Pliozän und Pleistozän in nord und mittel Chile unter besonderer Berücksichtigung der Entwicklung der Mollusken Faunen. Zitteliana 2, 1–159.

Higgs, R., 1979. Quartz-grain surface features of Mesozoic–Cenozoic sands from the Labrador and Western Greenland continental margins. Journal of Sedimentary Research 49, 599–610.

Hine, A.L., 1979. Mechanism of berm development and resulting beach growth along a barrier spit complex. Sedimentology 26, 333–351.

Jenny, B., Valero-Garcés, B.L., Villa-Martinez, R., Urrutia, R., Geyh, M.A., Veit, H., 2002. Early to mid-Holocene aridity in central Chile and the southern westerlies: the Aculeo Lake record (34°S). Quaternary Research 58, 160–170.

Jenny, H., 1941. Factors of Soil Formation: a System of Quantitative Pedology. McGraw-Hill, New York, USA.

Jenny, H., 1980. The Soil Resource—Origin and Behavior. Springer, New York.

Klappa, C.F., 1980. Brecciation textures and tepee structures in Quaternary calcrete (caliche) profiles from eastern Spain: the plant factor in their formation. Geological Journal 15, 81–89.

Krinsley, D.H., Donahue, J., 1968. Environmental interpretation of sand grain surface textures by electron microscopy. Geological Society of America Bulletin 79, 743–748.

Krinsley, D.H., Doornkamp, J.C., 1973. Atlas of Quartz Sand Surface Textures. Cambridge University Press.

Krischev, K.G., Georgiev, V.M., 1981. Surface textures of quartz grains as a source of information on sedimentation environment in the south Bulgarian Black Sea shelf. Geologica Balcanica 11, 77–99.

Kuenen, P.H.H., Perdok, W.G., 1962. Experimental abrasion 5. Frosting and defrosting of quartz grains. The Journal of Geology 70, 648–658.

Lamy, F., Hebbeln, D., Wefer, G., 1998. Late Quaternary precessional cycles of terrigenous sediment input off the Norte Chico, Chile (27.5°S) and palaeoclimatic implications. Palaeoecology Palaeoclimatology Palaeoecology 141, 233–251.

Le Roux, J.P., Olivares, D.M., Nielsen, S.N., Smith, N.D., Middleton, H., Fenner, J., Ishman, S.E., 2006. Bay sedimentation as controlled by regional crustal behaviour, local tectonics and eustatic sea-level changes: Coquimbo Formation (Miocene–Pliocene), Bay of Tongoy, central Chile. Sedimentary Geology 184, 133–153.

Loisy, C., Verrecchia, E.P., Dufor, P., 1999. Microbial origin for pedogenic micrite associated with a carbonate palaeosol (Champagne, France). Sedimentary Geology 126, 193–204.

Machette, M.N., 1985. Calcic soils of the southwestern United States. In: Weide, D.L. (Ed.), Soils and Quaternary Geology of the Southwestern United States, Geological Society of America Special Paper 203, pp. 1–21.

Mahaney, W.C., 2002. Atlas of Sand Grain Surface Textures and Applications. Oxford Universtiy Press, New York.

Maldonado, A., Villagrán, C., 2002. Palaeonvironmental changes in the semiarid coast of Chile (32°S) during the last 6200 cal years inferred from a swamp-forest pollen record. Quaternary Research 58, 130–138.

Maldonado, A., Villagrán, C., 2006. Climate variability over the last 9000 cal yr BP from a swamp forest pollen record along the semiarid coast of Chile. Quaternary Research 66, 246–258.

Margolis, S., Krinsley, D., 1974. Processes of formation and environmental occurrence of microfeatures on detrital quartz grains. American Journal of Science 274, 449–464.

Marquardt, C., Lavenu, A., Ortlieb, L., Godoy, E., Comte, D., 2004. Coastal neotectonics in southern central Andes: uplift and deformation of marine terraces in northern Chile (27°). Tectonophysics 394, 193–219.

McAuliffe, J.R., 1994. Landscape evolution, soil formation, and ecological patterns and processes in Sonoran Desert bajadas. Ecological Monographs 64, 111–148.

Meldahl, K., 1995. Pleistocene shoreline ridges from tide-dominated and wave-dominated coasts: northern Gulf of California and western Baja California, Mexico. Marine Geology 123, 61–72.

Melnick, D., Bookhagen, B., Echtler, H.P., Strecker, M.R., 2006. Coastal deformation and great subduction earthquakes, Isla Santa Maria, Chile (37°). GSA Bulletin 118, 1463–1480.

Navarro-Fernández, C.M., Aroca, R., Barea, J.M., 2011. Inlfuence of arbuscular mycorrhizal fungi and water regime on the development of endemic *Thymus* species in dolomitic soils. Applied Soil Ecology 48, 31–37.

Nelson, A.R., Manley, W.F., 1992. Holocene coseismic and aseismic uplift of Isla Mocha, south central Chile. Quaternary International 15/16, 61–76.

Olivares, D.M., 2004. Evolución Miocena-Pleistocena de las Sucesiones Sedimentarias Marinas de Bahía Tongoy. IV Región de Coquimbo. Memoria Geología, Universidad de Chile, Santiago, Chile.

Ota, Y., Miyauchi, T., Paskoff, R., Koba, M., 1995. Plio-Quaternary terraces and their deformation along the Altos de Talinay, north central Chile. Revista Geológica de Chile 22, 89–102.

Otvos, E.G., 2000. Beach ridges—definitions and significance. Geomorphology 32, 83–108.

Owen, J.J., Amundson, R., Dietrich, W.E., Nishiizumi, K., Sutter, B., Chong, G., 2011. The sensitivity of hillslope bedrock erosion to precipitation. Earth Surface Processes and Landforms 36, 117–135.

Paskoff, R., 1970. Recherches géomorphologiques dans le Chili semi-aride. Biscaye Freres, Bordeaux.

Pal, D.K., Kalbande, A.R., Deshpande, S.B., Sehgal, J.L., 1994. Evidence of clay illuviation on sodic soils of north-western part of the Indo-Gangetic plains since the Holocene. Soil Science 158, 465–473.

Pedoja, K., Regard, V., Husson, L., Martinod, J., Guillaume, B., Fucks, E., Iglesias, M., Weill, P., 2011. Uplift of Quaternary shorelines in eastern Patagonia: Darwin revisited. Geomorphology 127, 121–142.

Platt, N.H., 1989. Lacustrine carbonates and pedogenesis: sedimentology and origin of palustrine deposits from the Early Cretaceous Rupelo Formation, W Cameros Basin, N Spain. Sedimentology 36, 665–684.

Radtke, U., 1989. Marine Terrassen und Korallenriffe- das Problem der quartären Meeresspiegelschwankungen erläutert an Fallstudien aus Chile, Argentinien und Barbados. Düsseldorfer Gegographische Schriften Heft 27, Düsseldorf.

Ravelo, A.C., Andreasen, D.H., Lyle, A.O., Wara, M.W., 2004. Regional climate shifts caused by gradual global cooling in the Pliocene epoch. Nature 429, 263–267.

Reheis, M., 1987. Climatic implications of alternating clay and carbonate formation in semiarid soils of south-central Montana. Quaternary Research 27, 270–282.

Regard, V., Saillard, M., Martinod, J., Audin, L., Carretier, S., Pedoja, K., Riquelme, R., Paredes, P., Hérail, G., 2010. Renewed uplift of the Central Andes Forearc revealed by coastal evolution during the Quaternary. Earth and Planetary Science Letters 297, 199–210.

Please cite this article as: Pfeiffer, M., et al., Preservation of beach ridges due to pedogenic calcrete development in the Tongoy palaeobay, North-Central Chile, Geomorphology (2011), doi:10.1016/j.geomorph.2011.05.012

Rodbell, D.T., Seltzer, G.O., Andeson, D.M., Abott, M.B., Enfield, D.B., Newman, J.H., 1999. An ~15,000 year record of El Niño-driven alluviation in southwestern Ecuador. Science 283, 516–520.
Sadzawka, A., Carrasco, M.A., Grez, R., Mora, M.L., 2004. Métodos de Análisis Recomendados para los Suelos Chilenos. Comisión de Normalización y Acreditación, Sociedad Chilena de la Ciencia del Suelo.
Saillard, M., 2008. Dynamique du soulèvement côtier des Andes centrales: Etude de l'évolution géomorphologique et datations (10Be) de séquences de terrases marines (Sud Pérou-Nord Chili). PhD Thesis, Université de Touluse, France.
Sarkar, S., 1988. Petrology of caliche derived peloidal calcirudite/calcarenite in the late Triassic Maleri Formation of the Pranhita-Godavari Valley, south India. Sedimentary Geology 55, 263–282.
Schellmann, G., Radtke, U., 2010. Timing and magnitude of Holocene sea-level changes along the middle and south Patagonian Atlantic coast derived from beach ridge systems, littoral terraces and valley-mouth terraces. Earth Science Reviews 103, 1–30.
Schoenberger, P.J., Wysocki, D.A., Benham, E.C., Broderson, W.D., 2002. Field Book for Describing and Sampling Soils, Version 2.0. Natural Resources Conservation Service, National Soil Survey Center, Lincoln NE.
Siddall, M., Chappell, J., Potter, E.K., 2006. Eustatic sea-level during past interglacials. In: Sirocko, F., Litt, T., Claussen, M., Sanchez-Goni, M.F. (Eds.), The Climate of Past Interglacials. Elsevier, Amsterdam, pp. 75–92.
Stoops, G., 2003. Guidelines for Analysis and Description of Soil and Regolith in Thin Sections. Soil Science Society of America, Madison, USA.
Trewin, N., 1988. Use of the scanning electron microscope in sedimentology. In: Tucker, M. (Ed.), Techniques in Sedimentology. Blackwell Scientific Publications, Oxford, pp. 229–273.
VanArsdale, R., 1982. Influence of calcrete on the geometry of arroyos near Buckeye, Arizona. Geological Society of America Bulletin 93, 20–26.
Vargas, G., Rutlant, J., Ortlieb, L., 2006. ENSO tropical–extratropical climate teleconnections and mechanisms for Holocene debris flows along the hyperarid coast of western South America (17°–24°S). Earth and Planetary Science Letters 249, 467–483.
Veit, H., 1993. Upper Quaternary landscape and climate evolution in the Norte Chico (Northern Chile): an overview. Mountain Research and Development 13, 139–144.
Veit, H., 1996. Southern Westerlies during the Holocene deduced from geomorphological and pedological studies in the Norte Chico, Northern Chile (27–33°S). Palaeoecology Palaeoclimatology Palaeoecology 123, 107–119.
Vera, W., 1985. Mineralogy and micromorphology of calcium carbonate-rich soils from Chile. M.Sc. Thesis. State University of Ghent, Belgium.
Verrecchia, E.P., Verrechia, K.E., 1994. Needle-fiber calcite; a critical review and a proposed classification. Journal of Sedimentary Research 64, 650–664.
Verrechia, E.P., Dumont, J.L., 1996. A biogeochemical model for chalk alteration by fungi in semiarid environment. Biogeochemistry 35, 447–470.
Victor, P., Sobesiak, M., Glodny, J., Nielsen, S.N., Oncken, O., 2011. Long-term persistence of subduction earthquake segment boundaries—evidence from Mejillones Peninsula, N-Chile. Journal of Geophysical Research 116, B02402. doi:10.1029/2010JB007821.
Watts, N.L., 1977. Pseudo-anticlines and other structures in some calcretes of Botswana and South Africa. Earth Surface Processes and Landforms 2, 63–74.
Wells, S., McFadden, I., Dohrenwend, J., 1987. Influence of late Quaternary climatic changes on geomorphic and pedogenic processes on a desert piedmont, eastern Mojave Desert, California. Quaternary Research 27, 130–146.
Wright, V.P., 1990. A micromorphological classification of fossil and recent calcic and petrocalcic microstructures. In: Douglas, L.A. (Ed.), Soil Micromorphology: a Basic and Applied Science, Proceedings of the VIIIth International Working Meeting of Soil Micromorphology Developments in Soil Science 19. Elsevier, Amsterdam, pp. 401–407.
Wright, V.P., 1994. Paleosols in shallow marine carbonate sequences. Earth-Science Reviews 35, 367–395.
Wright, V.P., Wilson, R.C.L., 1987. A terra rosa like complex from the Upper Jurassic of Portugal. Sedimentology 34, 259–273.
Wright, V.P., Tucker, M.E., 1991. Calcretes: an introduction. In: Wright, V.P., Tucker, M.E. (Eds.), International Associaton of Sedimentology. Reprint Series, 2. Blackwell Scientific Publications, Oxford, pp. 1–22. Calcretes.
Wright, V.P., Mazzullo, S.J., Birdwell, B.A., 1990. Syngenetic formation of grainstones and pisolites from fenestral carbonates in peritidal settings: discussion. Journal of Sedimentary Research 60, 309–310.

Please cite this article as: Pfeiffer, M., et al., Preservation of beach ridges due to pedogenic calcrete development in the Tongoy palaeobay, North-Central Chile, Geomorphology (2011), doi:10.1016/j.geomorph.2011.05.012